Electrostrictive resonances in $(Ba_{0.7}Sr_{0.3})TiO_3$ thin films at microwave frequencies

S. Tappe,[a] U. Böttger, and R. Waser
Institut für Werkstoffe der Elektrotechnik 2, University of Aachen, D-52056 Aachen, Germany

(Received 24 November 2003; accepted 29 May 2004)

The bias-voltage-dependent permittivity of $(Ba_{0.7}Sr_{0.3})TiO_3$ (BST) thin films with thicknesses ranging from 100 to 250 nm is investigated in the frequency range from 500 MHz to 40 GHz by impedance spectroscopy of integrated BST capacitors. The dielectric spectra of the films exhibit resonance phenomena in the 4–7 GHz range when a bias field is applied. It is shown that the main controlling parameter of the resonance frequency is the film thickness. Calculations based on the strong electrostrictive activity of the BST films underline the assumption that the emission of plane acoustic waves is the underlying mechanism for this behavior. © *2004 American Institute of Physics*. [DOI: 10.1063/1.1775880]

Thin $(Ba_{0.7}Sr_{0.3})TiO_3$ (BST) films are being intensively studied for applications in voltage tunable high frequency devices like phase-shifters[1] or tunable filters.[2] In addition to the integration of these materials into existing device concepts their high frequency properties are still of major interest. Tunability, loss factor, temperature dependence, and dispersion characteristics are important aspects from the device point of view. It was shown that paraelectric BST thin films operate almost without dispersion up to *K* band fequencies at zero bias voltage.[3]

In ferroelectric bulk ceramics like barium titanate or lead titanate zirconate, however, a strong dielectric relaxation was observed in the GHz range during the last 50 years.[4] It is characterized by a decrease in the relative permittivity ε_r and a peak in the dielectric loss tan δ. Mechanisms attributed to these observations include piezoelectric resonance of grains and domains,[5] inertia to domain wall movement,[6] and the emission of gigahertz shear waves from ferroelastic domain walls.[7] As a result, the relaxation phenomenon appears to be intimately linked to the domain state of the ferroelectric. Arlt and co-workers quantitatively described this dispersion by the sound emission from vibrating 90° domain walls. The elastic medium on both sides of the domain wall with its mass and elastic properties is a quasi-infinite transmission line into which elastic shear waves are emitted. Above a certain frequency the emission of sound is suppressed and the domain walls no longer contribute to the dielectric response. McNeal *et al.* confirmed the model of shear sound emission by a systematic investigation of polycrystalline as well as composite barium titanate with different grain/particle sizes and domain states. In case of very fine grained samples, they even found a resonant behavior correlated to the piezoelectric activity of single domain grains.[8] For $LiNbO_3$ ceramics without any ferroelastic domain walls the dielectric behavior was modeled with an equivalent circuit of the grain resonances by Xi *et al.*[9] With this approach the dielectric spectrum of the ceramics could be predicted.

This letter reports about dielectric resonance phenomena in BST thin films which are observed while an electric bias field is applied. The dependence of the resonant frequency on the thickness and the temperature of the film is investigated. Calculations are carried out by means of an one-dimensional transmission line model, which considers the influence of the strong electrostrictivity, the geometry, and the material porperties of the BST film, the electrodes and the substrate.

Integrated $(Ba_{0.7}Sr_{0.3})TiO_3$ thin film capacitors with electrode areas from 2 μm×2 μm to 40 μm×40 μm and film thicknesses of 100, 150, 200, and 250 nm were fabricated on highly resistive silicon substrates ($\sigma > 10$ kΩ cm). Platinum (Pt) with a thickness of 100 nm was used as the bottom and top electrode material. The bottom electrodes and the BST films were structured by wet chemical etching. A lift-off technique was applied for pattering the top electrodes. X-ray diffraction analysis revealed good phase purity and a predominantly [110] orientation of the BST films. In the scanning electron microscope, the films appear dense with a columnar grain structure. The $C(f)$ curves reported in this letter have been measured with a HP8722ES network analyzer and Cascade Microtech Infinity probes for the on wafer probing of the sample capacitors. Open and short structures with the same geometry as the BST capacitors are used to correct for parasitic resistance, inductance, and capacitance. The calibration and deembeding of the analyzer and the probes were carried out with short, open, load, through (SOLT) on wafer standards of an ISS 190-101 impedance substrate (Cascade Microtech).

Figure 1(a) shows the capacitance spectrum of a $(Ba_{0.7}Sr_{0.3})TiO_3$ capacitor with a thickness of 200 nm. At zero bias voltage only little dispersion over the frequency range between 500 MHz and 40 GHz is noticed. With increasing the bias voltage the capacitance *C* decreases due to the tunability of the BST film. Additionally a slight relative increase of *C* at 4.3 GHz is followed by a drop to a lower level as the frequency rises. At the same time the loss tangent of the capacitor shows a peak as in Fig. 1(b). This and the slight increase of *C* before the drop reveal that the spectrum of the permittivity is related more to the resonant than the relaxation process. The difference of the capacitance before and after the resonance increases with increasing bias voltage U_{bias}, i.e., from 2% ($U_{bias}=1$ V) to 10% ($U_{bias}=10$ V). The resonance frequency (f_0) of 4.5 GHz itself remains constant for all bias voltages. This implies that a change of the dielectric constant has no impact on f_0. Virtually no temperature dependence of the resonance can be observed. The depen-

[a]Electronic mail: tappe@iwe.rwth-aachen.de

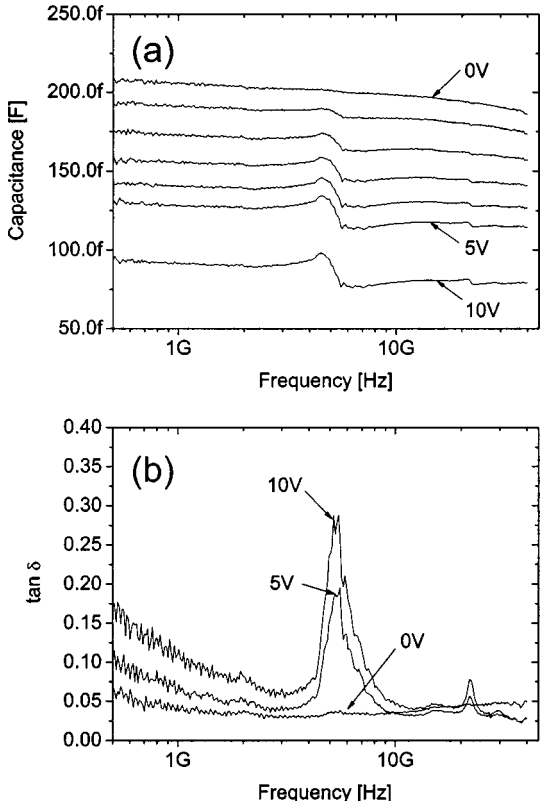

FIG. 1. Capacitance (a) and loss factor (b) over frequency of a 4 μm $\times 4$ μm $(Ba_{0.7}Sr_{0.3})TiO_3$ capacitor (thickness 200 nm) at bias voltages from 0 to 10 V. From 0 to 5 V the voltage is increased in 1 V steps.

dence of f_0 on the film thickness h_{BST} is plotted in Fig. 2. With increasing h_{BST} the resonance frequency decreases. Thus, the film thickness is the controlling parameter of the resonance. The described resonance phenomena repeats at around 21 GHz. It is known that bulk acoustic waves form inside a piezoelectric plate due to electro-mechanical coupling. If the plate is bounded by air or vacuum the generated waves stay confined inside the material. The resonant frequencies of this thickness mode correspond to odd multiples of a half acoustic wavelength across the plate and can be calculated as a function of the plate/film thickness h_{film}, the mass density ρ, and the velocity of sound v:

$$f_0 = \frac{nv}{2h_{\mathrm{film}}}. \tag{1}$$

Although BST thin films are paraelectric at room temperature, their strong electrostrictive behavior enables the emis-

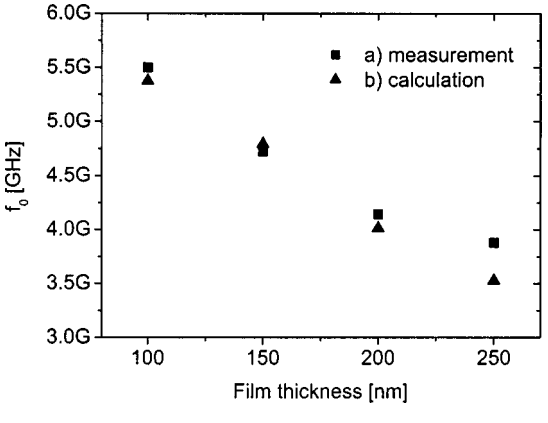

FIG. 2. Resonance frequency of the fundamental mode vs film thickness: (a) measurement, (b) calculation.

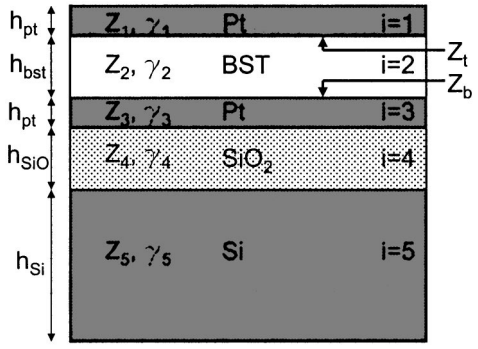

FIG. 3. Schematic of all material layer of the capacitor and their corresponding acoustic properties.

sion of bulk acoustic waves.[10] Therefore it is assumed that the BST thin film acts as a transducer element, which converts electrical energy into plane longitudinal acoustic waves traveling through the BST film, the top and bottom electrode, and the substrate material. Thus, any resonance phenomena are determined through the acoustic properties and the dimension of each material layer incorporated in the BST capacitor. In Fig. 3 each material layer i of the BST capacitor is assigned to an acoustic impedance $Z_i = \rho_i v_i$ and a phase delay $\gamma_i = \omega h_i / v_i$ where ω is the angular frequency, ρ_i the mass density, v_i the sound velocity, and h_i the height. The sound velocity depends on the mode of the acoustic wave that is traveling through the medium. For a plane longitudinal wave, v_i is given by[11]

$$v_i = \sqrt{(\lambda_i + \mu_i)/\rho_i}. \tag{2}$$

The two Lamé constants λ_i and μ_i can be derived from Young's modulus E_i and Poisson's ratio σ_i:

$$E_i = (\mu_i(3\lambda_i + 2\mu_i))/(\lambda_i + \mu_i), \tag{3}$$

$$\sigma_i = (\lambda_i)/(2(\lambda_i + \mu_i)). \tag{4}$$

The impedance spectrum of the BST capacitor can be calculated if the electrostrictive coupling is related to the sound propagation. With the piezoelectric coupling coefficient $k = \sqrt{d^2 E_2/(\epsilon_0 \epsilon_r)}$, where d is the piezoelectric coefficient, and the capacitance $C = \epsilon_0 \epsilon_r A / h_2$, the electric input impedance of the BST film bounded by the two acoustic impedances z_t and z_b can be written as[12]

$$Z_{\mathrm{in}} = \frac{-j}{\omega C}\left(1 - \frac{k^2}{\gamma_2}\frac{(z_t + z_b)\sin\gamma_2 + 2j(1-\cos\gamma_2)}{(z_t + z_b)\cos\gamma_2 + j(1 + z_t z_b \sin\gamma_2)}\right). \tag{5}$$

The bounding impedances $z_t = Z_t/Z_2$ and $z_b = Z_b/Z_2$ can be derived by using transmission line theory.[13] Z_{top} is the transformation of the impedance Z_∞ of the surrounding medium (air/vaccum) through the acoustic transmission line formed by the top electrode:

$$Z_t = jZ_1 \tan\gamma_1. \tag{6}$$

Similarly, the acoustic impedance Z_b is the transformation of Z_∞ through the silicon substrate (layer $i=5$), the silicondioxide (layer $i=4$), and the platinum bottom electrode (layer $i=3$):

$$Z_b = j\frac{Z_{sb}\tan\gamma_{sb} + Z_3\tan\gamma_3}{1 - (Z_{sb}/Z_3\tan\gamma_3\tan\gamma_{sb})}, \tag{7}$$

TABLE I. Material properties of layer *i* shown in Fig. 3.

Layer	Material	ρ(kg/m^3)	E(GPa)	E''/E'	σ	1(10^{-9} m)
1,3	Pt	21 090	168	0.05	0.38	100
2	BST	5 596	125[a]	0.05	0.3[a]	100–250
4	SiO_2	2 200	73	0.05	0.17	450
5	Si	2 330	150	0.05	0.17	455×10^3

[a]Reference 14.

$$Z_{sb} = \frac{j(Z_5 \tan \gamma_5 + Z_4 \tan \gamma_4)}{1 + Z_5/Z_4 \tan \gamma_4 \tan \gamma_5}. \quad (8)$$

With the combination of Eqs. (2)–(8) and the material parameters of Table I the capacitance spectrum of a 250 nm BST capacitor is calculated and plotted in Fig. 4, where graph (a) corresponds to the measurement and (b) to the calculation. A good agreement between the measurment and the modeling can be observed, although the calculated resonant frequencies are slightly lower than the measured values. A better fit can be obtained, if the values of Young's modulus of the BST and the Pt layer are increased by 10% [Fig. 4(c)]. It must be noted that a complex value is used for Young's modulus $E_i = E_i' - jE_i''$ in order to acount for mechanical losses. The ratio of the imaginary and real parts is given in Table I. In addition, the calculated thickness dependence of the first resonant frequency is plotted in Fig. 2 and again agrees well with the values determined by the experiment.

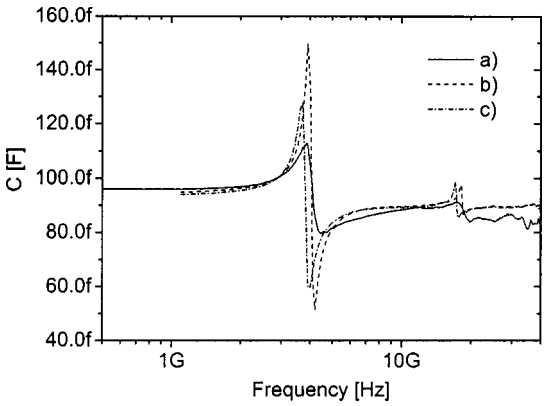

FIG. 4. Measured and calculated capacitance spectrum of 250 nm BST capacitor: (a) measurement, (b) calculation with values according to Table I, d=15 pm/V and ϵ_r=105, (c) calculation with E_1, E_2, and E_3 10% higher than given in Table I.

In conclusion, the high frequency properties of BST thin films with an applied electrical bias field are presented. The films exhibit thickness-dependent characteristic resonances in the GHz frequency range. It is demonstrated that sound emission due to the strong electrostrictive behavior of the BST film is the underlying mechanism of the presented phenomena. Analytical calculations based on a transducer model and transmission line theory show a good prediction of the capacitance spectrum and the thickness dependence of the resonance.

[1]A. Nagra and R. A. York, IEEE Trans. Microwave Theory Tech. **47**, 1705 (1999).
[2]I. Vendik, O. Vendik, V. Pleskachev, A. Svishchev, and R. Wördenweber, IEEE MTT-S Int. Microwave Symp. Dig. **3**, 1461 (2001).
[3]J. D. Baniecki, R. B. Laibowitz, T. M. Shaw, P. R. Duncombe, D. A. Neumayer, D. E. Kotecki, H. Shen, and Q. Y. Ma, Appl. Phys. Lett. **72**, 498 (1998).
[4]A. von Hippel, Rev. Mod. Phys. **22**, 221 (1950).
[5]A. von Hippel, Z. Phys. **133**, 158 (1952).
[6]C. Kittel, Phys. Rev. **83**, 458 (1951).
[7]G. Arlt, U. Böttger, and S. Witte, Ann. Phys. (Leipzig) **3**, 578 (1994).
[8]M. P. McNeal, S. Jang, and R. E. Newnham, J. Appl. Phys. **83**, 3288 (1998).
[9]Y. Xi, H. McKinstry, and L. Cross, J. Am. Ceram. Soc. **66**, 637 (1983).
[10]W. P. Mason, Phys. Rev. **B74**, 1134 (1948).
[11]W. P. Mason, *Physical Acoustics and the Properties of Solids* (van Nostrand, New York, 1958)
[12]E. Sittig, Phys. Acoust. **9**, 221 (1972).
[13]H. B. O. Zinke, *Lehrbuch der Hochfrequenztechink* (Springer, Berlin, 1986), Chap. 2.2.
[14]G. Mader, H. Meixner, and P. Kleinschmidt, J. Appl. Phys. **58**, 702 (1985).